

Studies of Metallofullerene Primary Soots by Laser and Thermal Desorption Mass Spectrometry

L. Moro,*† R. S. Ruoff,* C. H. Becker, D. C. Lorents,* and R. Malhotra

Molecular Physics Department, SRI International, 333 Ravenswood Ave., Menlo Park, California 94025

Received: March 4, 1993; In Final Form: April 8, 1993

Laser desorption (LD) and thermal desorption (TD) mass spectra of the metallofullerenes found in arc-produced primary soots have been studied for a large variety of alkaline earth and lanthanide elements. The metallofullerene ratios found in the LD spectra indicate that two distinct groups are observed: Sc, Y, La, Ce, Pr, Nd, Gd, Tb, Ho, Er, and Lu (group A) and Ca, Sr, Sm, Eu, and Yb (group B). The TD spectra of most of these same soots also separate into two groups that contain the same elements as groups A and B. Group A metallofullerenes show strong signals in both LD and TD spectra. Group B metallofullerenes are distinguished by their presence in the LD spectra but absence in the TD spectra. From the general ionic behavior of the elements of these groups, and recent studies of the endohedral oxidation states, we propose that the oxidation states are +3 for group A and +2 for group B. C_{70} metallofullerenes are anomalous in that they are absent in TD spectra for all group A and B elements, even at $T = 750$ °C, but present in LD spectra.

Introduction

Metallofullerenes were first made in molecular beams in 1985 by Smalley's group at Rice University.¹ La-loaded graphite was laser ablated and examined in an ion cyclotron resonance mass spectrometer (ICR), and mass peaks with the stoichiometry of LaC_{2n} were observed. In 1988, clever "shrink wrapping" experiments showed that the photoexcited LaC_{2n} shrank by sequential C_2 loss until a cutoff mass was reached and that the cutoff mass was a function of the ionic radius.² These experiments provided convincing evidence that in metal atom-carbon clusters produced in this manner the metals (La, K, Cs) were enclosed within the fullerene cage. The name *endohedral* was suggested³ to designate a fullerene with an atom or ion inside it, and the currently employed symbol for an endohedral is $M@C_{2n}$, indicating that M is encaged by C_{2n} .⁴ The molecular beam method was used to demonstrate that endohedral metallofullerenes can be formed with alkalis, alkaline earths, lanthanides, and uranium.⁵ This work stimulated a number of theoretical calculations of the electronic structure of the endohedrals,^{3,6-8} all of which suggested that encaged metals can be ionized, their ionic state depending on the interaction of the atomic valence and the fullerene cage electrons. For example, the early calculation of Rosén and Wästberg on $La@C_{60}$ predicts a charge of +2.85 on the encaged La^6 corresponding to a formal charge of +3. However, other calculations indicated much lower charge levels for the encaged metal.⁷

The arc production method discovered in 1990^{9,10} led to large-quantity production of fullerenes and has been the focus of recent efforts to produce useful quantities of endohedrals. Graphite rods loaded with metal oxides have been vaporized in high-current arcs in a He environment at low pressure.¹¹⁻²⁰ Mass spectrometry of the soot produced under these conditions clearly shows the presence of metallofullerenes of C_{2n} over a large range of n . The existence of $M_2@C_{2n}$ and $M_3@C_{2n}$ has also been observed for several metals. Efforts to chemically extract the metallofullerenes from the fullerene soot have unfortunately met with very limited success. Only $M@C_{82}$ is readily extracted by solvents, although metallofullerenes with more than one metal atom appear to be more readily extracted.¹⁹

It has been possible to concentrate enough $M@C_{82}$ in a fullerene extract to measure its electron spin resonance (ESR) spectrum.

ESR measurements on endohedrals of La, Y, and Sc show the metal to be in the +3 oxidation state in every case.¹²⁻¹⁵ Indeed, the lanthanide and actinide elements are very electropositive.²¹ Raymond and Eigenbrot²² have analyzed a wide range of organolanthanide and organoactinide crystals and found that the bond distances can be predicted to within 0.01 Å if entirely ionic bonding is assumed. Assuming only ionic bonding for $M@C_{60}$, Wang et al.²³ used the ionization potentials of atoms and electron affinities of C_{60} to predict $M@C_{60}$ stabilities and metal ion oxidation states for a large range of metals. A very recent structural calculation on $M@C_{82}$ predicts a charge state of +3 for La, with its minimum energy position being off center.²⁴ Thus, the oxidation states of the metal atoms in these endohedrals seem reasonably well established and in accord with what is to be expected for lanthanide and actinide elements.

The determination of the oxidation state and stability of the endohedral fullerenes is a problem of considerable scientific and practical importance. By analogy with the well-studied A_3C_{60} crystalline materials, which behave as metals and low-temperature superconductors when A is an alkali,²⁵ it is possible that endohedrals with triply charged ions will have similar properties. In the alkali intercalated fullerites, three electrons populate a half-filled (LUMO) of the fullerene, leading to a partially filled conduction band in the crystal. Similarly, it is possible that crystalline endohedrals with the enclosed M in the +3 oxidation state will behave as metals and even superconductors. The possibility that stable fullerite conductors and superconductors could be fabricated from endohedrals is very tantalizing and justifies studies into methods for efficient production of them.

We present here a study of a range of metals that form metallofullerenes by the arc synthesis method and examine their production and thermal stability characteristics. A major fraction of the lanthanides as well as selected group IIa and IIIb elements were examined. The endohedral-containing soots were examined by postionization mass spectrometry using laser and thermal decomposition methods to vaporize the fullerenes. Laser desorption postionization mass spectrometry (SALI, surface analysis by laser ionization)²⁶ provides a meaningful measure of the nascent concentrations of all of the fullerenes in the soot because of the rapid desorption of the material. The slower thermal desorption process provides a measure of the thermal stability of individual metallofullerenes in addition to the desorption temperatures. The systematics of these results over a large range of metallofullerenes strongly suggests two groupings based on the oxidation state of the encaged atom. The thermal desorption experiments also

* Authors to whom correspondence should be addressed.

† Visiting scientist from Istituto per la Ricerca Scientifica e Tecnologica, Divisione di Scienza dei Materiali, I-38050 Povo-Trento, Italy.

suggest this process as a possible method for separation of endohedrals from soot and from C_{60} and larger empty fullerenes. Although we have not demonstrated that the metallofullerenes observed in this study are really endohedrals, nevertheless we use the nomenclature of $M@C_{2n}$ to designate them.

Experimental Section

The primary goal of this study was to survey metallofullerene products from arc-produced carbon soot. To make a comparison of metallofullerene product distributions meaningful, primary (raw) metal-containing soots were derived in as reproducible a fashion as possible. A dc arc was employed, with a stationary 12.7-mm-diameter graphite negative electrode and an 8-mm-diameter translating positive graphite electrode (Advanced Carbon AC-8, Brisbane, CA). A 23-cm-deep, 3.2-mm-diameter hole was drilled in the 30.5-cm-long positive electrode and packed with metal oxide powder (Johnson-Mathey, Reacton grade, -35 mesh). The atomic ratio of metal to carbon in the packed portion of the rod was approximately 0.02. Two mixed-metal runs were performed, the first involving a 1:1 (by weight) mixture of Lu_2O_3 and La_2O_3 and the second a 1:1 (by weight) mixture of Sm_2O_3 and La_2O_3 . The corresponding metal atomic ratios are approximately 0.82:1 (Lu:La) and 0.93:1 (Sm:La). These mixed-metal runs, where arc conditions have to be identical, were done as a check on the reproducibility of arc conditions for the monometal runs. The positive graphite electrode was coupled to a stainless steel rod that was itself coupled to a translation stage maintained under computer control. A geared-down dc electric motor maintained constant rotation of the graphite electrode as it was translated into the chamber. A computer controlled the feed rate via a stepper motor-driven linear translation stage. Current and temperature was also monitored by computer-interfaced sensors on the chamber. The positive electrode was advanced until the arc was struck and then retracted by computer control of the translation stage to maintain a constant gap of 5 mm. The arc was imaged onto a calibrated screen so that the gap between electrodes could be accurately determined. The current was held at 150 A and the voltage at about 30 V. The typical feed rate for the translating positive electrode was 0.1 mm/s, which was substantially higher than is used for solid graphite rods not packed with metal oxide powder.

The base pressure of the fullerene chamber prior to a run was 0.020 mbar, and the chamber was purged twice with Ar and then pressurized to 250 mbar with He. The He was flowed in a horizontal collection tube at a rate of about 50 sccm, and entrained soot was collected directly into a large Soxhlet thimble (Whatman single thickness, 60 mm \times 180 mm cellulose extraction thimble), with pumping by a mechanical pump. After the discharge was turned off, the chamber was brought slowly to atmospheric pressure by first leaking air to about 50 mbar with continuous pumping. This exposure to a low-pressure air environment was maintained for about 1 h to oxidize any remaining metal before the chamber was opened to the atmosphere and the soot collected in the thimble removed for analysis.

Two different types of desorption were used in this study, laser desorption (LD) and temperature-programmed thermal desorption (TPD). For LD-SALI analysis the primary soot was pressed into indium foil and introduced into the vacuum apparatus (10^{-9} mbar). The SALI technique has been previously described.²⁶ Briefly, neutrals desorbed from a sample were photoionized by a laser beam passing 1 mm above and parallel to the sample surface. The photoions were mass analyzed by a reflecting time-of-flight mass spectrometer and detected by a dual-microchannel plate assembly. Laser desorption with pulsed 532-nm light from a Nd:YAG laser was used to obtain the relative concentrations of the different fullerenes and metallofullerenes in the primary soot. The desorbing laser power was maintained at low enough levels such that no fullerene fragments or directly produced ions were detected (about 10 mJ/cm² in 5-ns pulses).

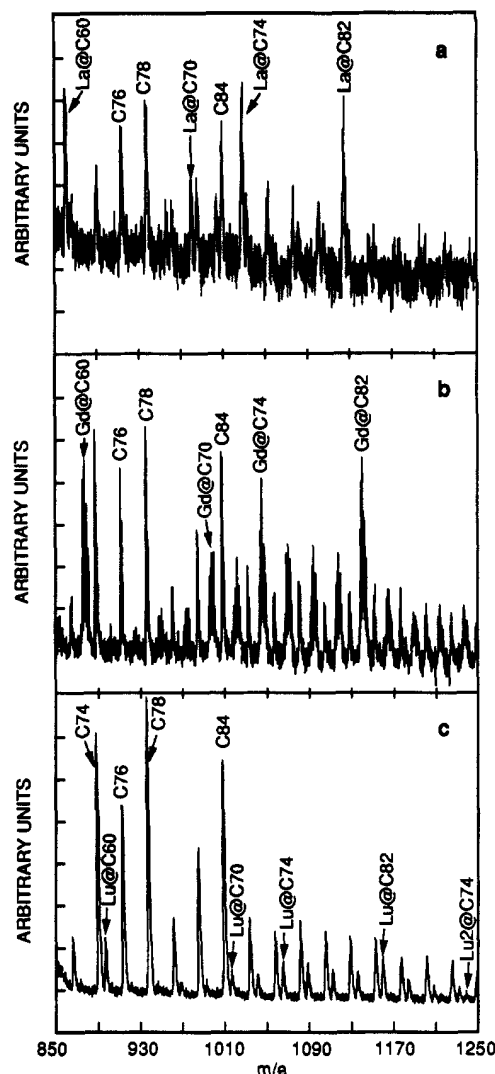


Figure 1. LD-SALI mass spectra of (a) La, (b) Gd, and (c) Lu primary soots in the mass range 850–1250 amu. The major fullerene and metallofullerene peaks are labeled. Note that the intensities of $M@C_{74}$ and $M@C_{82}$ are on the same order as that of $M@C_{60}$. In the Gd case, the peaks are broadened by the isotopic distribution of Gd.

Thermal desorption was achieved with a resistively heated sample holder controlled by a microprocessor (Model 808, Eurotherm, Reston, VA), with the temperature monitored by a Chromel–Alumel thermocouple. The soot was held in place with a fine mesh copper net which was in good thermal contact with the sample holder. The TPD data cover the range 25–750 °C, with ramp rates ranging from 10 to 90 °C/min. In some cases, complete mass spectra as a function of temperature were obtained, while in other cases the integrated signal profiles for several masses were acquired as a function of temperature.

Photoionization was achieved with 118-nm light (10.5-eV photon energy), the ninth harmonic of the Nd:YAG, by a single-photon process. The photoionization cross sections of the fullerenes and metallofullerenes are assumed to be the same for these above-threshold photons, based on observations of ionization efficiencies for other large molecules.²⁷ Therefore, observed intensities are expected to be fairly accurate representations of the actual number concentrations of desorbing species.

Results and Discussion

LD spectra for primary soots containing La, Gd, and Lu are shown in Figure 1. The mass range 850–1250 Da shown in Figure 1 includes the metallofullerenes that are the subject of this study. With La as an example, the lowest mass metallofullerene observed

TABLE I: Peak Height Ratios $M@C_{2n}:M@C_{60}$

element	$M@C_{70}$	$M@C_{74}$	$M@C_{82}$
Group A			
Sc	0.4	0.6	0.6
Y	0.4	0.6	1.0
La	0.6	1.3	1.3
Ce	0.4	0.4	0.4
Pr	0.2	0.4	0.4
Nd	0.6	0.6	0.6
Gd	0.5	1.0	1.4
Tb	0.4	0.4	0.4
Ho	0.4	0.4	0.4
Er	0.5	0.7	0.8
Lu	0.5	0.7	0.9
Group B			
Sm	0.2	0.1	0.1
Eu	0.2	<0.1	<0.1
Yb	0.3	<0.1	<0.1
Ca	0.3	0.2	0.1
Sr	0.4	0.2	0.2

is $La@C_{60}$, which is adjacent to the fullerene C_{74} . The next metallofullerene is $La@C_{66}$, followed by a series of $La@C_{2n}$ that extends to masses as large as the highest fullerene mass observed, C_{128} . As observed by others,^{11,16} $La@C_{70}$ is more prominent than its neighbors, $La@C_{68}$ and $La@C_{72}$, but $La@C_{74}$ and $La@C_{82}$ are more intense than $La@C_{70}$. The relative spectral intensities of metallofullerenes from several different samples of La soot were reproducible to within 25%.

Under our experimental conditions, monometallofullerenes are primarily produced. However, in the case of Lu, dimetallofullerenes such as $Lu_2@C_{74}$ are observed (see Figure 1c). This production of dimetallofullerenes may be due to Lu^{3+} (0.861 Å) having a smaller ionic radius than La^{3+} (1.032 Å).¹⁹ Dimetallofullerenes were also seen for the primary Sc soot, which is not displayed in Figure 1. When the isotopic distribution of Gd (which produces the broad peaks observed for $Gd@C_{2n}$) was accounted for, the Gd metallofullerenes were observed to be the most abundant of all the lanthanide endohedrals produced under our conditions. For example, the $Gd@C_{74}:C_{60}$ ratio is 0.05, while the $La@C_{74}:C_{60}$ ratio is 0.025.

The elements which exhibited prominent $M@C_{60}$, $M@C_{70}$, $M@C_{74}$, and $M@C_{82}$ peaks with comparable intensities to those depicted in Figure 1 are La, Gd, Lu, Ce, Pr, Nd, Tb, Ho, Sc, Y, and Er. The similarities are more clearly indicated in Table I, which lists the peak height ratios $M@C_{2n}:M@C_{60}$. As group A in Table I shows, the ratio of $M@C_{74}$ or $M@C_{82}$ to $M@C_{60}$ is typically equal to or larger than the ratio of $M@C_{70}$ to $M@C_{60}$.

LD-SALI spectra for primary soots containing Ca, Eu, and Sm are shown in Figure 2. $M@C_{60}$ is again the lowest mass metallofullerene observed, followed by $M@C_{66}$. In contrast to the situation in Figure 1, the intensity of metallofullerenes is monotonically decreasing as a function of mass, and $M@C_{74}$ and $M@C_{82}$ are weak compared to $M@C_{60}$. Sr and Yb exhibited spectra similar to those in Figure 2. As can be seen in Table I, in contrast to the case for group A, the ratios for $M@C_{74}$ and $M@C_{82}$ in group B are all less than that for $M@C_{70}$. Thus, the metallofullerenes examined here behave in their mass dependence as two distinct classes (groups A and B).

LD-SALI spectra of two mixed-metal primary soots showed the same metallofullerene distributions as the distributions from the single-metal soots. For example, the Sm/La primary soot showed Sm and La distributions identical to those of the individual Sm and La primary soots. The same was true of the mixed-metal La/Lu primary soot. The LD-SALI spectrum of the La/Lu primary soot showed that La is substantially more favored than Lu in formation of metallofullerenes, the ratio of $La@C_{60}$ to $Lu@C_{60}$ being about 3 to 1 (with similar ratios for other $La@C_{2n}$

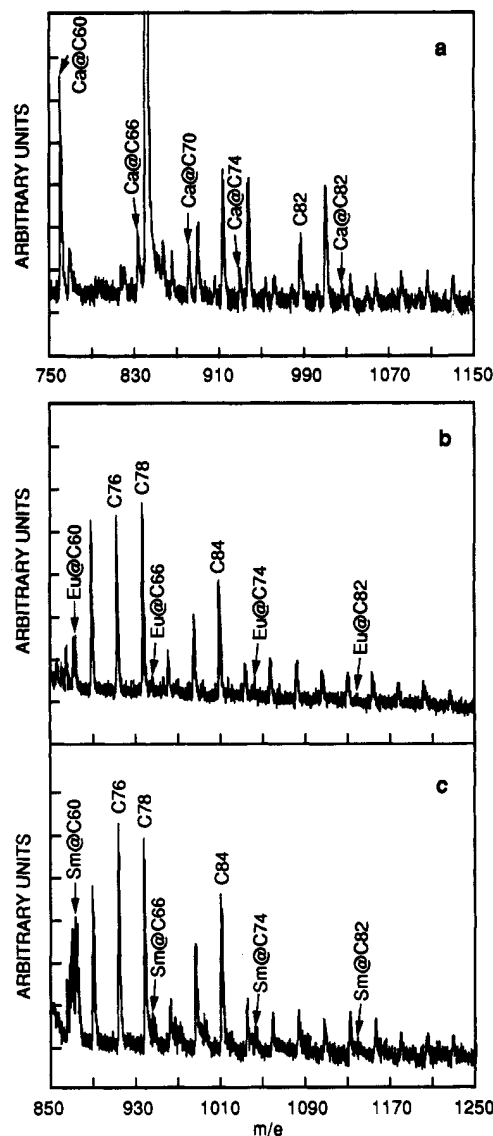


Figure 2. LD-SALI mass spectra of (a) Ca, (b) Eu, and (c) Sm primary soots. Note that, in contrast to Figure 1, the metallofullerene peak intensities strongly decrease with increasing mass.

and $Lu@C_{2n}$ species). Given that the starting atomic ratio of Lu to La is about 0.82, the arc synthesis method employed here favors formation of La metallofullerenes by about a factor of 2.5.

The temperature-programmed desorption (TPD) profiles of C_{60} and $La@C_{60}$ in Figure 3 show a striking difference in the thermal desorption kinetics of the empty C_{60} and metallo- C_{60} . This finding suggests that the $M@C_{60}$ is more strongly bound to the soot particles than C_{60} . The TPD profiles of all of the metallofullerenes, including $M@C_{60}$, are quite similar to those of the larger empty fullerenes, such as C_{78} and C_{84} . Thus, the larger metallofullerenes such as $M@C_{82}$ appear to desorb in the same temperature range as their parent fullerenes. Due to limitations in the temperature range of these TPD experiments, we were unable to obtain the complete TPD profile for the larger fullerenes and metallofullerenes, and therefore the data we report here are thermal desorption spectra for $T \leq 750$ °C.

Figure 4 shows thermal desorption (TD) spectra of La primary soot at four different temperatures for the mass range 850–1150 Da. C_{76} first starts to desorb at about 420 °C (not shown), and evidence of metallofullerenes desorption occurs at about 500 °C, when $La@C_{60}$ first appears. $La@C_{74}$ and $La@C_{82}$ become apparent at about 550 °C. Spectrum b in Figure 4 shows the fullerene and metallofullerene intensities at 620 °C. The main

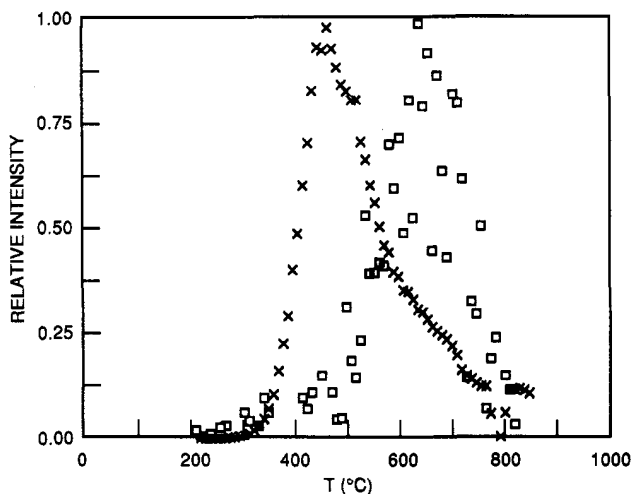


Figure 3. TPD spectra of C_{60} (X) and $La@C_{60}$ (□) from La primary soot. Note that the $La@C_{60}$ peak is similar in shape to that of C_{60} but is shifted toward higher temperatures. Higher mass metallofullerenes desorb at temperatures slightly higher than $M@C_{60}$ but in the same range as the large regular fullerenes.

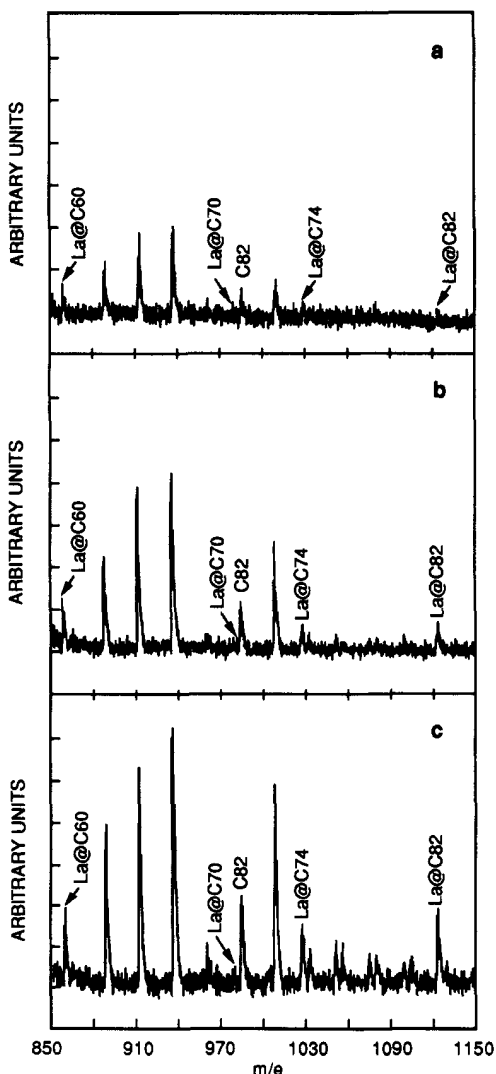


Figure 4. TD spectra of La primary soot at (a) 550 °C, (b) 620 °C, and (c) 750 °C. The ramp rate used for these measurements was 50 °C/min.

fullerene peaks (namely C_{74} , C_{76} , C_{78} , and C_{84}), are present, and $La@C_{60}$, $La@C_{74}$, and $La@C_{82}$ are clearly detectable. The $La@C_{70}$ Δ peak is notably absent. The metallofullerene peaks grow in intensity with increasing temperature, and at 750 °C the

TABLE II: Presence of $M@C_{2n}$ in TPD Spectra^a

	Y	La	Pr	Gd	Lu	Ho	Tb	Sm	Ca	Sr
$M@C_{60}$	Y,w	Y	Y,w	Y	Y	Y	Y	N	N	N
$M@C_{70}$		N	N	N	N	N	N	N	N	N
$M@C_{74}$	Y	Y	Y	Y	Y	Y,w	Y	N	N	N
$M@C_{76}$		Y,w	Y,w	Y	Y	Y,w	Y	N	N	N
$M@C_{80}$				Y	Y			N	N	N
$M@C_{82}$	Y	Y	Y	Y	Y	Y	Y	N	N	N
$M_2@C_{74}$					Y					
$M_2@C_{80}$					Y					
$M_2@C_{82}$					Y					
$M_2@C_{84}$					Y					

^a Y indicates $M@C_{2n}$ is present, and N indicates it is not. w indicates a weak peak intensity.

$La@C_{76}$, $La@C_{78}$, $La@C_{80}$, and $La@C_{82}$ signals are strong. In stark contrast to the LD spectra, where the $La@C_{70}$ intensity was comparable to that of its close neighbor, C_{82} , as well as to those of $La@C_{76}$ and $La@C_{78}$, the TD spectra show $La@C_{70}$ to be essentially absent at all temperatures, even at 750 °C. Other elements that exhibit TD spectra similar to those of Figure 4 are Y, Pr, Gd, Tb, Ho, and Lu. TD-SALI spectra for Nd, Er, and Ce were not recorded. For Lu primary soot, $Lu@C_{74}$ and $Lu_2@C_{74}$, as well as $Lu@C_{82}$ and $Lu_2@C_{82}$, were observed to desorb at essentially the same temperature.

In contrast to the case for elements listed above, TD-SALI spectra recorded for Ca, Sr, and Sm soots showed no metallofullerene signals at any temperature up to 750 °C. Only empty fullerenes were observed to desorb in this temperature range. These same soots showed strong metallofullerene signals in the LD spectra. This contrasting behavior suggests that these species are thermally unstable under thermal desorption conditions, where the time for reaction is much longer than that under laser desorption conditions.

Table II summarizes the results of the TD measurements of metallofullerenes from primary soots. Again we find that the elements fall into two classes: those that desorb metallofullerenes and those that do not. Remarkably, these two groups contain the same elements as the groups A and B found in the LD-SALI spectra. The elements of group A behave very similarly to each other but very differently than those of group B, both in their nascent metallofullerene distributions and in their thermal desorption properties. Table II also shows the remarkable absence of $M@C_{70}$ of all M examined by thermal desorption.

ESR studies of $M@C_{82}$ by Johnson et al.¹² and others¹³⁻¹⁵ indicate that La, Y, and Sc are all present as M^{3+} , and this oxidation state is confirmed by recent detailed calculations for the La case.²⁴ The oxidation state of these metals in the other $M@C_{2n}$ is presently not known. It is known that La almost always is present in nature in the +3 oxidation state,²⁸ and the few exceptions involve very unstable compounds. One might, therefore, expect that all of the $La@C_{2n}$ will have La present as La^{3+} . Gd, Lu, Sc, and Y are also elements that are almost always in the +3 oxidation state, and in fact most of the other lanthanide elements follow this trend.²⁸ The most stable +2 lanthanide is Eu, followed by Yb and Sm. It is well-known that the alkaline earth elements Ca, Sr, and Ba are very electropositive and are always present in the +2 oxidation state. Recently, Smalley and co-workers²⁹ studied the negative ion detachment spectroscopy of $Ca@C_{60}^-$ and concluded that for $Ca@C_{60}^-$ the Ca has transferred two electrons to the C_{60} cage. The *ab initio* calculations of Scuseria³⁰ agree that the charge state of Ca for the endohedral $Ca@C_{60}$ is 2+. All of this evidence leads us to propose that the group A and group B metallofullerenes found in the LD-SALI and TD-SALI spectra correspond to the metals with +3 and +2 oxidation states, respectively; i.e., in the metallofullerenes, the group A elements (Sc, Y, La, Ce, Pr, Nd, Gd, Tb, Ho, Er, and Lu) are in the +3 oxidation state and the group B elements (Ca, Sr, Sm, Eu, and Yb) are in the +2 oxidation state.

Conclusions

Laser desorption and thermal desorption mass spectra of the metallofullerenes found in reproducible arc-produced primary soots have been studied for a variety of alkaline earth and lanthanide elements. The LD-SALI spectra can be classified into two groups based on metallofullerene ratios. Group A comprises Sc, Y, La, Ce, Pr, Nd, Gd, Tb, Ho, Er, and Lu, and group B comprises Ca, Sr, Sm, Eu, and Yb. TD-SALI spectra of most of these same soots also reveal two groups, which contain the same members as groups A and B. On the basis of the general ionic behavior of the elements of these groups, the recent results for $\text{Ca}@C_{60}^{29}$ and $\text{M}@C_{2n}^{12-15}$ and *ab initio* calculations^{6,24} of the oxidation states of $\text{M}@C_{2n}$, we propose that these groups are distinguished by the oxidation state of the encaged metal, namely, +3 for group A and +2 for group B. This assignment, which is based on indirect evidence, needs corroboration by more direct measurements.

TPD-SALI spectra of group A primary soots show that C_{60} desorbs at lower temperatures than $\text{La}@C_{60}$ and that $\text{La}@C_{74}$ and $\text{La}@C_{82}$ desorb at only slightly higher temperatures than $\text{La}@C_{60}$. Elements that behave like $\text{La}@C_{2n}$ in their TD-SALI spectra are in group A. However, TD-SALI spectra of primary soots of the group B elements show only empty fullerenes desorbing as a function of temperature, up to 750 °C. The metallofullerenes of group B, which are clearly seen in the LD-SALI spectra, either are thermally unstable or do not desorb at temperatures of ≤ 750 °C. However, since they are desorbed by low-flux laser desorption, the more probable explanation is that they are thermally unstable in this environment. $\text{M}@C_{70}$ is anomalous in that it is absent in TD-SALI spectra for all group A elements, even at 750 °C, but strongly present in LD-SALI spectra. This finding implies that $\text{M}@C_{70}$ is less thermally stable than the other metallofullerenes and behaves in a manner similar to that of the group B elements.

Acknowledgment. Lorenza Moro acknowledges the financial support of the Italian CNR (Centro Nazionale per le Ricerche). We gratefully acknowledge the contributions of Mark Dyer, who developed the arc computer-interfaced controls and sensors, and the technical assistance of Bryan Chan and Donald Keegan. We appreciate useful discussions with John Callahan and Mark Ross of the Naval Research Laboratory. Part of this work was conducted under the program "Advanced Chemical Processing Technology", consigned to the Advanced Chemical Processing Technology Research Association from the New Energy and Industrial Technology Development Organization, which is carried out under the Large-Scale Project administered by the Agency of Industrial Science and Technology, the Ministry of International Trade and Industry, Japan.

Note Added in Proof. Recent interpretation of temperature dependence of ESR spectra has led Kato and co-workers³¹ to conclude that $\text{Sc}@C_{82}$ has Sc present in the +2 rather than +3 oxidation state, in contradiction to our pairing of Sc with La (which is +3) rather than with Ca, based on LD-SALI spectra. We point out that Sc metallofullerene soots were *not* studied by

the TD-SALI technique employed for most primary metallofullerene soots of the present study, due to low S/N in the LD-SALI spectra. We feel, therefore, that the case of Sc merits, in particular, further study.

References and Notes

- Heath, J. R.; O'Brien, S. C.; Zhang, Q.; Liu, Y.; Curl, R. F.; Kroto, H. W.; Smalley, R. E. *J. Am. Chem. Soc.* **1985**, *107*, 7779.
- Weiss, F. D.; O'Brien, S. C.; Elkind, J. L.; Curl, R. F.; Smalley, R. E. *J. Am. Chem. Soc.* **1988**, *110*, 4464.
- Cioslowski, J.; Fleischmann, E. *J. Chem. Phys.* **1991**, *94*, 3730.
- Nomenclature $\text{M}@C_{2n}$ attributed to O. Cheshnovsky, as mentioned in ref 11.
- Guo, T.; Diener, M. D.; Alford, M. J.; Haufler, R. E.; McClure, S. M.; Ohno, T.; Weaver, J. H.; Scuseria, G. E.; Smalley, R. E. *Science* **1992**, *257*, 1661 and references therein.
- Rosén, A.; Wästberg, B. *J. Am. Chem. Soc.* **1988**, *110*, 8701. Rosén, A.; Wästberg, B. *Z. Phys. D: At., Mol. Clusters* **1989**, *12*, 387.
- Chang, A. H. H.; Ermler, W. C.; Pitzer, R. M. *J. Chem. Phys.* **1991**, *94*, 5004.
- Cioslowski, J. *J. Am. Chem. Soc.* **1991**, *113*, 4139.
- Kratschmer, W.; Lamb, L. D.; Fostiropoulos, K.; Huffman, D. R. *Nature* **1990**, *347*, 354.
- Haufler, R. E.; Conceicao, J.; Chibante, L. P. F.; Chai, Y.; Byrne, N. E.; Flanagan, S.; Haley, M. M.; O'Brien, S. C.; Pan, C.; Xiao, Z.; Billups, W. E.; Ciufolini, M. A.; Hauge, R. H.; Margrave, J. L.; Wilson, L. J.; Curl, R. F.; Smalley, R. E. *J. Phys. Chem.* **1990**, *94*, 8634.
- Chai, Y.; Guo, T.; Jin, C.; Haufler, R. E.; Chibante, L. P. F.; Fure, J.; Wang, L.; Alford, J. M.; Smalley, R. E. *J. Phys. Chem.* **1991**, *95*, 7564.
- Johnson, R. D.; de Vries, M. S.; Salem, J. R.; Bethune, D. S.; Yannoni, C. S. *Nature* **1992**, *355*, 239.
- Shinohara, H.; Sato, H.; Saito, Y.; Ohkohchi, M.; Ando, Y. *J. Phys. Chem.* **1992**, *96*, 3571.
- Yannoni, C. S.; Hoinkis, M.; de Vries, M. S.; Bethune, D. S.; Salem, J. R.; Crowder, M. S.; Johnson, R. D. *Science* **1992**, *256*, 1191.
- Shinohara, H.; Sato, H.; Ohkohchi, M.; Ando, Y.; Kodama, T.; Shida, T.; Kato, T.; Saito, Y. *Nature* **1992**, *357*, 52.
- Ross, M. M.; Nelson, H. H.; Callahan, J. H.; McElvany, S. W. *J. Phys. Chem.* **1992**, *96*, 5231.
- Ruoff, R. S.; Malhotra, R.; Moro, L.; Becker, C. H.; Lorents, D. C. In Proceedings of the Symposium on Novel Forms of Carbon. *Mater. Res. Soc. Symp. Proc.* **1992**, *270*, 249.
- Alvarez, M. M.; Gillan, E. G.; Holczer, K.; Kaner, R. B.; Min, K. S.; Whetten, R. L. *J. Phys. Chem.* **1991**, *95*, 10561.
- Gillan, E. G.; Yerezian, C.; Min, K. S.; Alvarez, M. M.; Whetten, R. L.; Kaner, R. B. *J. Phys. Chem.* **1992**, *96*, 6869.
- Hoinkis, M.; Yannoni, C. S.; Bethune, D. S.; Salem, J. R.; Johnson, R. D.; Crowder, M. S.; de Vries, M. S. *Chem. Phys. Lett.* **1992**, *198*, 461.
- CRC Handbook of Chemistry and Physics*, 73rd ed.; CRC Press: Boca Raton, FL, 1992; pp 4-121.
- Raymond, K. N.; Eigenbrot, Jr., C. W. *Acc. Chem. Res.* **1980**, *13*, 276.
- Wang, Y.; Tomanek, D.; Ruoff, R. *Chem. Phys. Lett.*, in press.
- Laasonen, K.; Andreoni, W.; Parinello, M. *Science* **1992**, *258*, 1916.
- Hebard, A. F.; Rosseinsky, M. J.; Haddon, R. C.; Murphy, D. W.; Glarum, S. H.; Palstra, T. T. M.; Ramirez, A. P.; Kortan, A. R. *Nature* **1991**, *350*, 600. Ruoff, R. S.; Wang, Y.; Tomanek, D. *Chem. Phys. Lett.* **1993**, *203*, 438. Hebard, A. *Phys. Today* **1992**, *45*, 26 and references therein.
- Becker, C. H.; Gillen, K. T. *Anal. Chem.* **1984**, *56*, 1671. Schüle, U.; Pallix, J. B.; Becker, C. H. *J. Am. Chem. Soc.* **1988**, *110*, 2323.
- Reid, N. W. *Int. J. Mass Spectrom. Ion Phys.* **1971**, *6*, 1.
- Cotton, S. *Lanthanides and Actinides*; Oxford University Press: New York, 1991.
- Wang, L. S.; Alford, J. M.; Chai, Y.; Diener, M.; Zhang, J.; McClure, S. M.; Guo, T.; Smalley, R. E.; Scuseria, G. E. *Chem. Phys. Lett.*, in press.
- Scuseria, G. Abstract presented at the 182nd Electrochemical Society Meeting, Fullerenes: Chemistry, Physics, and New Directions III Symposium, Toronto, Oct. 11, 1992; abstract 765.
- Kato, T.; Nagase, S.; Suzuki, S.; Kikuchi, K.; Achiba, Y. S8.2, MRS 1993 Spring Meeting, San Francisco, 1993.